Chemistry
A European
Journal

Chemistry Europe
European Chemical Societies Publishing

Accepted Article

Title: Conformationally Restricted β-Sheet Breaker Peptides Incorporating Cyclic α-Methylisoserine Sulfamidates

Authors: Nuria Mazo, Claudio D. Navo, Francesca Peccati, Jacopo Andreo, Cristina Airoldi, Gildas Goldsztejn, Pierre Çarçabal, Imanol Usabiaga, Mariona Sodupe, Stefan Wuttke, Jesús H. Busto, Jesús M. Peregrina, Emilio J. Cocinero, and Gonzalo Jiménez-Osés

To be cited as: *Chem. Eur. J.* **2022**, e202202913

Link to VoR: https://doi.org/10.1002/chem.202202913

WILEY-VCH

10.1002/chem.202202913

WILEY-VCH

Conformationally Restricted β-Sheet Breaker Peptides Incorporating Cyclic α-Methylisoserine Sulfamidates

Nuria Mazo,[a,b] Claudio D. Navo,[c] Francesca Peccati,[c] Jacopo Andreo,[d] Cristina Airoldi,[e] Gildas Goldsztejn,[f] Pierre Çarçabal,[f] Imanol Usabiaga,[g,h] Mariona Sodupe,[i] Stefan Wuttke,[d,j] Jesús H. Busto,[a] Jesús M. Peregrina,[a] Emilio J. Cocinero*[g,h] and Gonzalo Jiménez-Osés*[a,c,j]

Dedicated to Prof. Dr. Joan Bosch on the occasion of his 75th anniversary

[a] Dr. Nuria Mazo, Dr. Jesús H. Busto, Prof. Dr. Jesús M. Peregrina, Dr. Gonzalo Jiménez-Osés
Departamento de Química
Universidad de La Rioja, Centro de Investigación en Síntesis Química
26006 Logroño, Spain
[b] Dr. Nuria Mazo: 3P Biopharmaceuticals, 31110 Noáin, Navarra, Spain.
[c] Dr. Claudio D. Navo, Dr. Francesca Peccati, Dr. Gonzalo Jiménez-Osés
Computational Chemistry Lab
Center for Cooperative Research in Biosciences (CIC bioGUNE), Basque Research and Technology Alliance (BRTA)
Bizkaia Technology Park, Building 800, 48160 Derio, Spain
Email: gjoses@cicbiogune.es
https://www.cicbiogune.es/people/gjoses
[d] Dr. Jacopo Andreo, Dr. Stefan Wuttke
BCMaterials, Basque Center for Materials
UPV/EHU Science Park, Leioa 48940, Spain
[e] Dr. Cristina Airoldi
BioOrgNMR Lab, Department of Biotechnology and Biosciences
University of Milano-Bicocca
Piazza della Scienza, 2, 20126 Milano, Italy
[f] Dr. Gildas Goldsztejn, Dr. Pierre Çarçabal
Institut des Sciences Moléculaires d'Orsay (ISMO), Université Paris Saclay, CNRS
91405, Orsay, France
[g] Dr. Imanol Usabiaga, Dr. Emilio J. Cocinero
Departamento de Química Física, Facultad de Ciencia y Tecnología
Universidad del País Vasco (UPV/EHU)
48080 Bilbao, Spain
Email: emiliojose.cocinero@ehu.eus
[h] Dr. Imanol Usabiaga, Dr. Emilio J. Cocinero
Instituto Biofisika (CSIC, UPV/EHU)
48080 Bilbao, Spain
[i] Prof. Dr. Mariona Sodupe
Departament de Química
Universitat Autònoma de Barcelona
08193 Bellaterra, Spain
[j] Dr. Stefan Wuttke, Dr. Gonzalo Jiménez-Osés
Ikerbasque, Basque Foundation for Science
48009 Bilbao, Spain

Supporting information for this article is given via a link at the end of the document.

Abstract: Peptides containing variations of the β-amyloid hydrophobic core and five-membered sulfamidates derived from β-amino acid α-methylisoserine have been synthesized and fully characterized in the gas phase, solid state and in aqueous solution by a combination of experimental and computational techniques. The cyclic sulfamidate group effectively locks the secondary structure at the N-terminus of such hybrid peptides imposing a conformational restriction and stabilizing non-extended structures. This conformational bias, which is maintained in the gas phase, solid state and aqueous solution, is shown to be resistant to structure templating through assays of *in vitro* β-amyloid aggregation, acting as β-sheet breaker peptides with moderate activity.

Introduction

Cyclic sulfamidates are well-known electrophiles, commonly used as building blocks to synthesize various chemicals and biomolecules.[1–9] Particularly, chiral five-membered ring sulfamidates derived from hydroxy-α- and β-amino acids have been extensively used as precursors of chemically modified amino acids.[10–17] The reactivity of sulfamidate-containing peptides has been extensively studied,[11] including short peptides incorporating α-methylisoserine-derived sulfamidate by our group.[18–21] However, although such chiral scaffolds can be regarded as structural analogs of cyclic amino acids (Pro or βPro),[22,23] their structural properties have been much less explored. Analysis of reported crystallographic[18,24] and quantum mechanical[25] structures reveals that amide-substituted α-methylisoserine sulfamidates show highly conserved conformational features, particularly at the C-terminal amide bond. We envisioned that these structural preferences, which

mainly originate from an electrostatic interaction between the amide N-H and sulfamidate endocyclic O atoms,[25] could be transferred to small peptides incorporating such chiral and conformationally restricted motif. To test this hypothesis, we incorporated α-methylisoserine sulfamidate **1** into the β-amyloid (Aβ) hydrophobic core (**Aβ17-21**) in an attempt to produce a so-called β-sheet breaker peptide[26–33] (BSBP, Figure 1) for the inhibition of Aβ aggregation.

BSBPs specifically bind to Aβ blocking and/or reversing its aggregation into β-sheet-rich oligomers and insoluble deposits. Soto and co-workers pioneered the BSBP strategy by developing compound **2** (Ac-Leu-Pro-Phe-Phe-Asp-NH_2), a small peptide able to both inhibit amyloid aggregation and disrupt preformed fibrils,[26,27] in which the β-sheet stabilizing valine[34] in **Aβ17-21** is replaced by a proline[35] (Figure 1). Proline is an innate β-sheet breaker residue owing to its cyclic structure,[22,36] and is often found in β-turn motifs. Based on this strategy, several BSBP candidates containing cyclic unnatural residues have been developed, particularly hybrid α/β-peptides incorporating homoproline (β-HPro),[37] anthranilic acid (Ant)[38] and N-terminal sulfonamide derivatives (i.e. containing taurine) (Figure 1).

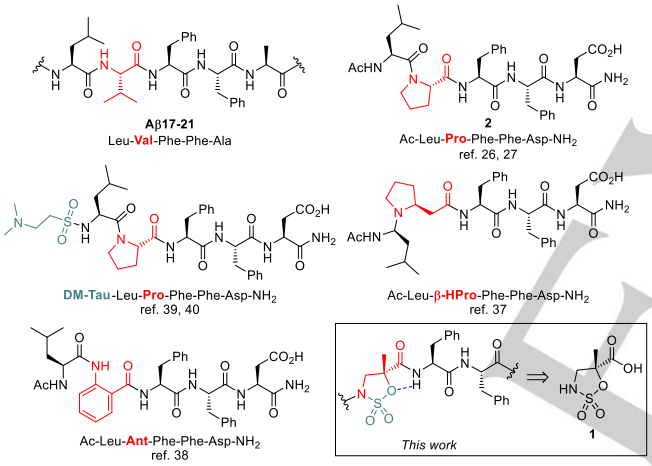

Figure 1. Structures of Aβ hydrophobic core and different β-sheet breaker peptides (BSBP) comprising cyclic α- and β-amino acids and sulfonamides, including the minimal motif incorporating α-methylisoserine sulfamidate **1** (inset) presented in this work.

We envisaged that a similar β-sheet breaking effect might be exerted by the peptide's N-terminus backbone conformation – induced by the sulfamidate moiety– which does not match the backbone dihedral distribution of a β-strand. This mismatch weakens the hydrogen bond pattern of the growing β-sheet architecture and prevents recruitment of further Aβ monomeric units. Of note, it has been suggested that the sulfonamide moiety contributes to inhibit aggregation by altering polarity and hydrogen bonding patterns.[39,40] Our sulfamidate moiety **1** is likewise cyclic, and in addition features a sulfamate motif likely engaged in an intra-molecular interaction[25] which entails an enthalpic penalty to flexibility (see dashed blue line in Figure 1).

Here, we present a multi-disciplinary strategy for the development and complete structural analysis of small peptides incorporating cyclic α-methylisoserine sulfamidates, by combining solid-phase synthesis, high-resolution IRID spectroscopy, X-ray crystallography, circular dichroism, NMR spectroscopy, computer modeling and *in vitro* activity. Some of these compounds showed a comparable or even larger anti-aggregation activity than proline when embedded in the same peptide sequence. Finally, a model for amyloid inhibition mechanism is proposed.

Results and Discussion

Synthesis of BSBPs. To minimize the issues associated to the synthesis of small peptides incorporating sulfamidate **1** in solution,[18–20] the coupling of this scaffold to longer peptides was optimized using microwave-assisted solid-phase synthesis (MW-SPPS, Scheme 1).[21] First, Fmoc-protected amino acids were consecutively attached to a Rink amide MBHA resin using the standard coupling-deprotection protocol. N-unprotected sulfamidate **1** could be then coupled directly since the reactivity at its quaternary center (i. e. ring-opening or elimination reactions) is silenced in the absence of an activating group.[20,25] Several parameters for the synthesis of peptide **3-resin** were optimized (SI Table S1), noting that microwave assistance is pivotal for the coupling to proceed. Part of the resin was treated with the cleavage cocktail to release the peptide from the resin and remove the protecting groups, obtaining peptide **3**. Fmoc-protected leucine was then coupled to peptide **3-resin** either at low temperatures to avoid the ring-opening of the N-functionalized (i.e. activated) sulfamidate with nucleophilic coupling reagents, or with microwave activation using non-nucleophilic coupling reagents (SI Table S2), to obtain peptide **4** after cleavage.

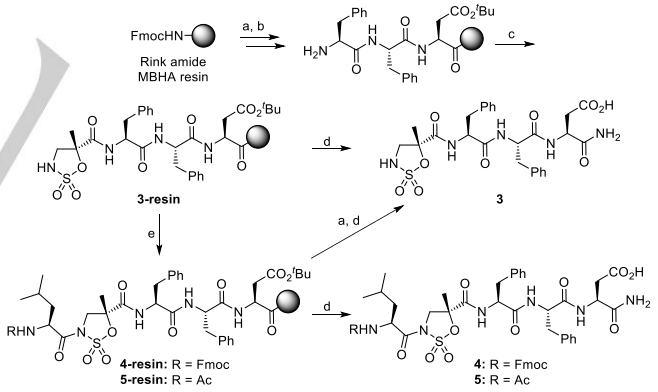

Scheme 1. Synthesis of peptides containing α-methylisoserine-derived sulfamidate **1**. *Reagents and conditions:* a) 20% (v/v) piperidine in DMF for Fmoc deprotection; b) Fmoc-protected amino acid (5 equiv.), Oxyma Pure®, DIC, and DMF for coupling natural amino acids; c) **1** (5.0 equiv.), Oxyma Pure® (5.5 equiv.), DIC (20 equiv.), DMF, 75 ºC (MW), 20 min; d) TFA/TIS/H_2O (95:2.5:2.5), 25 °C, 1 h; e) Fmoc-Leu-OH, DIPEA (5.5 equiv.), DIC (20 equiv.), DMF, 75 °C (MW), 20 min for peptide **4**, or Ac-Leu-OH, DIPEA (5.5 equiv.), DIC (20 equiv.), DMF, 25 °C, 16 h for peptide **5**.

However, the final substitution of the N-terminal Fmoc by an acetyl group could not be achieved under any of the many conditions assayed (SI Table S3), obtaining always deacylated peptide **3** as a sole product upon Fmoc deprotection. Alternatively, *N*-acetyl-leucine was coupled to peptide **3-resin** (Scheme 1). Unfortunately, although this strategy did allow obtaining peptide **5** after cleavage, two epimers in a 1:3 ratio at the terminal leucine were detected and separated by HPLC, despite using very mild conditions for the coupling (25 °C without

microwave irradiation); this undesired epimerization reaction is commonly used when coupling *N*-acetyl amino acids.[41] Additionally, when peptide **5** was dissolved in aqueous phosphate-buffered saline (PBS, pH 7.5), the N-terminal leucine was again cleaved to form peptide **3**, as confirmed by NMR, MS and HPLC. Therefore, and although compound **5** would be directly comparable to Soto's BSBP **2**, it was finally discarded for further studies due to the lack of complete stereochemical assessment and, more importantly, its instability in solution.

We then proceeded to synthesize a small library of peptides containing the sulfamidate moiety at the N-terminal position, either unprotected or capped as *N*-acetylsulfamate, and featuring Soto's FFD (peptides **3** and **6**) and the longer native **Aβ17-21** sequences (peptides **7** and **8**) (Table 1). For comparison, full-length Soto's BSSP and shorter analogues containing a proline instead of the cyclic sulfamidate (**2**: Ac-LPFFD-NH_2, **9**: Ac-PFFD-NH_2, and **10**: Ac-PFFAE-NH_2), as well as the minimal **1**-Phe-Phe-NH_2 motif (peptide **11**) were also synthetized.

Table 1. Synthesized sulfamidate and proline-containing peptides.

Peptide	Sequence	Global yield (%)[a]
2	Ac-Leu-Pro-Phe-Phe-Ala-Glu-NH_2	80
3	**1**-Phe-Phe-Asp-NH_2	72
6	Ac-**1**-Phe-Phe-Asp-NH_2	51
7	**1**-Phe-Phe-Ala-Glu-NH_2	62
8	Ac-**1**-Phe-Phe-Ala-Glu-NH_2	49
9	Ac-Pro-Phe-Phe-Asp-NH_2	71
10	Ac-Pro-Phe-Phe-Ala-Glu-NH_2	65
11	**1**-Phe-Phe-NH_2	75

[a] Yield calculated as mmol of HPLC-purified peptide divided by mmol of resin labelling content.

Conformational analysis of sulfamidate-containing peptides in the gas phase. In an attempt to elucidate the intrinsic conformational preferences of these sulfamidate-containing peptides, we first studied the gas phase structural properties of the **1**-Phe-Phe-NH_2 motif (peptide **11**), conserved in all sulfamidate containing peptides studied here. To this end, conformer-specific and mass-resolved infrared double resonance ion-dip (IRID) spectroscopy was used. This strategy allows the structural characterization of small-to-medium sized molecules and the precise study of inherent intramolecular interactions without interference from surrounding species in condensed media (i.e. aqueous solvents), and has been successfully employed to deduce the gas phase conformational preferences of several biomolecules.[42–45] In particular, amide N–H stretching vibrational modes are very sensitive to the strength and pattern of hydrogen bonds, thus providing information about the low-energy conformations (i.e. folding) adopted by small peptides in the absence of solvent effects. For tripeptide **11**, an intense absorption band at around 3150 cm^{-1}, three overlapping bands in the 3350–3450 cm^{-1} region, and one distinct band at around 3500 cm^{-1} are observed (Figure 2).

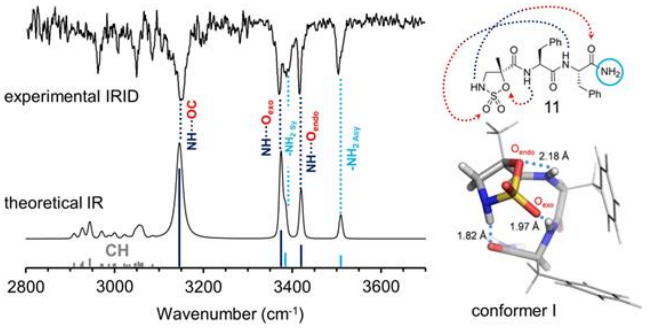

Figure 2. Top panel: Experimental infrared ion-dip (IRID) spectrum of peptide **11** in the gas phase. Lower panel: Calculated N–H vibrations for lowest-energy conformer **I**. The high correspondence between calculated and observed bands is highlighted with dotted lines. (Right panel) Three-dimensional structure calculated for conformer **I** with B3LYP-D3/6-311++G(2d,p). Hydrogen bonds are highlighted with dotted lines.

The presence of such well-resolved and separated bands suggests that only one conformer is present at IRID. The sharp peaks of the REMPI 1+1' (SI Figure S2) spectrum also suggest this trend. The infrared frequencies calculated for the lowest-energy conformer **I** (see SI and Table S4) shown in Figure 2 almost perfectly match those measured experimentally, indicating that such arrangement is the most populated one in the gas phase. Conformers **III**-**V** calculated quantum mechanically for peptide **11** are all very similar both structurally (i.e. they all are folded) and spectroscopically (SI Figure S3-S5) and could have a residual contribution in the IRID spectrum. The major conformer **I** exhibits a completely folded secondary structure as a result of an intricate hydrogen bond network involving the sulfamidate N–H, O_{exo} and O_{endo} atoms (Figure2). As previously reported,[25] the tertiary α-methyl group of the sulfamidate moiety plays a decisive role to lock the amide bond in a very stable and unusual arrangement ($\psi_\beta \approx -137°$). As a result of this conformational lock, the Phe residue attached to the sulfamidate (*i*+1 position) is stabilized in an α-helix conformation ($\varphi_\alpha \approx -62°$, $\psi_\alpha \approx -34°$) through the direct N-H to O_{endo} interaction, and the consecutive terminal Phe (*i*+2 position) folds into an inverse γ-turn conformation ($\varphi_2 \approx -78°$, $\psi_2 \approx +89°$) through hydrogen bonds between its C=O and N–H groups with sulfamidate N–H and O_{exo} groups, respectively. The non-extended orientation of the two Phe side chains (g^-, $\chi^1{}_\alpha \approx +50°$ for Phe1; g^+, $\chi^1{}_2 \approx -62°$ for Phe2) creates a hydrophobic patch through aromatic C–H/π interactions between the two nearly perpendicular phenyl rings which encapsulate one the two sulfamidate O_{exo} groups. This confirms our initial hypothesis that this densely functionalized five-membered cyclic amino acid confers strong bias towards novel non-extended conformations[46–48] to small peptides in which it is incorporated, with high potential for disrupting extended β-sheet structures such as those present in amyloid fibrils.

Structure of sulfamidate-containing peptides in the solid state. The next step in assessing the conformational preferences of peptides featuring sulfamidate **1** was to determine their structure in the solid state. Fortunately, peptide **11** could be crystallized layering its solution in acetone with hexane (see SI and Table S5). X-ray diffraction analysis of the obtained monocrystals revealed that traces of water co-crystallized with the substrate in a 1:2 stoichiometry (**11**·2H_2O) create a dense intermolecular hydrogen-bond network involving

the sulfamidate and amide groups (Figure 3). These water molecules intercalate between the sulfamidate and amide atoms previously described to form direct hydrogen bonds in the gas phase (Figure 2), yielding a less compact structure (solvent excluded surface area = 378 Å^2 in the solid state versus 341 Å^2 in the gas phase; probe radius 1.4 Å), although a very similar folded secondary structure was observed. The sulfamidate moiety retained the same geometry and hydrogen bond pattern involving its NH and oxygen atoms, and the tertiary amide was also locked in the same unusual conformation ($\psi_\beta \approx -133°$) due to the presence of the α-methyl group and the conserved N–H to O_{endo} interaction. Both phenylalanine residues showed α-helix conformations, the first Phe being slightly distorted from the canonical dihedral angles ($\varphi_\alpha \approx -123°$, $\psi_\alpha \approx +19°$ for Phe1; $\varphi_2 \approx -55°$, $\psi_2 \approx -42°$ for Phe2). In contrast with the gas-phase conformation, the sidechains of both Phe residues adopted an extended arrangement to maximize packing with other peptide molecules in the crystal (*g*$^+$, $\chi^1_\alpha \approx -57°$ for Phe1; *t*, $\chi^1_2 \approx -176°$ for Phe2). Of note, a clear intramolecular C-H/π interaction between the α-methyl group of the sulfamidate and the phenyl ring of Phe1 was observed.

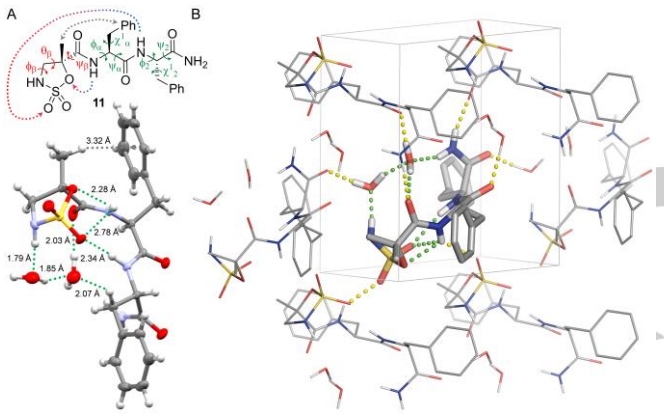

Figure 3. X-ray structure of peptide **11**, including two co-crystallized water molecules (**11**·2H$_2$O). A) ORTEP diagram showing thermal ellipsoids at the 50% probability level. B) Crystal packing showing the asymmetric unit cell (gray box). Intra- and intermolecular polar interactions within the molecules in the unit cell (shown in sticks) are shown as green dashed lines; interactions with molecules outside the unit cell are shown as yellow dashed lines.

The non-covalent intermolecular interactions between peptide units in the crystal structure were analyzed quantum mechanically by subtracting from the charge density of the bulk that of a fictitious crystal of non-interacting molecules (see SI). As expected, two main types of non-covalent interactions that alternate along crystallographic direction *a* were detected: hydrogen bonds involving the polar N-terminus of the peptide and co-crystallized water molecules at higher densities, and weaker van der Waals interactions involving phenylalanine side chains at lower densities (SI Figure S6).

Conformational analysis of sulfamidate-containing peptides in solution. The conformational preferences of peptides **3** and **6**–**10** in aqueous solution were first studied by circular dichroism (CD) (Figure 4). As expected, CD spectra suggest that longer peptides have a slightly better-defined structure than shorter variants. Of note, the characteristic β-sheet profile was not observed for any of them. Instead, a polyproline-II helix-like conformation is preferred in all cases.

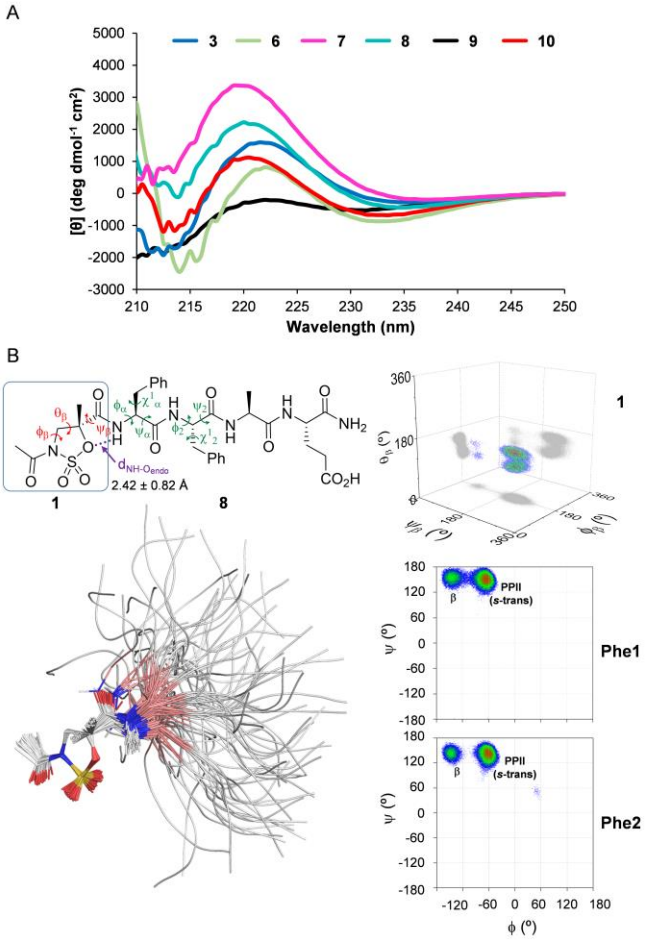

Figure 4. Conformational analyses of sulfamidate-containing and natural peptides in aqueous solution. A) CD spectra for 500 µM solutions of peptides **3** and **6**–**10** in PBS (50 mM, pH 7.4). B) 100 snapshots ensemble extracted from MD-tar simulations (500 ns) of sulfamidate-containing peptide **8**. Sulfamidate **1** is shown as lines. Natural amino acids are shown as light gray ribbon, and the (*i*+1) Phe residue as pale pink ribbon. Average distance between the endocyclic oxygen of the sulfamidate and the NH of the Phe residue (dNH–O_{endo}), three-dimensional plots of torsional angle distributions (ϕ_β, ψ_β, θ_β) around the sulfamidate moiety, and two-dimensional plots of torsional angle distributions (ϕ, ψ) of the Phe residues are shown. In the three-dimensional plots, torsional angle distributions are shown from 0° to 360° as colored spheres and projections onto each axis are shown as grey dots. In the two-dimensional plots, the torsional angle distribution are shown from -180° to +180° as colored dots. Colors range from densely populated (*i.e.* stable, Δ*E* = 0.0-1.0 kcal mol^{-1}, red-green) to scarcely populated (*i.e.* unstable, Δ*E* ≥ 1.0-2.0 kcal mol^{-1}, blue-white) structures.

2D-NOESY NMR experiments and molecular dynamics simulations with time-averaged restraints (MD-tar) were combined to obtain a detailed representation of the secondary structure of sulfamidate-containing peptides **3** and **6**–**8** in aqueous solution (see SI). Experimental distances were deduced from 2D-NOESY cross-peak intensities and were used as geometrical restrains in the MD-tar simulations. Average distances obtained from the simulations were consistent with the experimental ones, confirming that such calculations are able to correctly capture the structural behavior of these peptides in water (SI Figure S7). As observed in the gas phase and solid state for the minimal **1**-Phe-Phe sequence, the ψ_β dihedral angle is locked between –120° and –150° and the interaction between the amide N–H of the *i*+1 residue (Phe) and the endocyclic oxygen (O_{endo}) of the sulfamidate is conserved for all peptides also in water (averaged distance ~2.4 Å, Figure 4B and SI

Figure S8-S11). Variable-temperature ^{1}H NMR experiments suggested that such interaction might not be a canonical hydrogen bond, in agreement with its geometrical features derived from the MD-tar simulations (SI Figure S13). The terminal *N*-acetylsulfonamide in peptides **6** and **8** is locked into a *cis* amide bond disposition as confirmed by medium-size NOE cross-peaks (Ac–H_{proR} and Ac–H_{proS}), which differs from the normal *trans* preference in α-proline, and resembles the behavior observed for β-proline.[49,50]

The conformational bias imposed by the cyclic sulfamidate is transferred to the adjacent amino acids, highlighting the sulfamidate's ability to tune the peptide's secondary structure. Particularly, the *i*+1 Phe residue predominantly displays a folded polyproline-II helix conformation in all studied peptides (PP-II, $\varphi_\alpha \approx -60°$, $\psi_\alpha \approx +150°$), with minor populations of extended β-strand conformations (β, $\varphi_\alpha \approx -150°$, $\psi_\alpha \approx +150°$, Figure 4B). These conformational preferences resemble those described for residues adjacent to cyclic amino acids, e.g. residues preceding a proline.[51] On the other hand, the propensity to adopt PP-II-type conformations decreases with increasing distance from the N-terminal sulfamidate (SI Figure S12). These conformational preferences agree with the CD experiments, which showed a preponderance of folded PP-II-like conformations in water solution, and hinder the formation of β-sheet structures such as those occurring at the LVFF hydrophobic core in Aβ.

***In vitro* amyloid inhibition activity**. The kinetics of $A\beta_{1\text{-}40}$ aggregation in the presence of sulfamidate-containing peptides **3**, and **6**–**8** were monitored and compared to those of proline-containing peptides **2**, **9**, and **10**. These experiments were performed *in vitro* using thioflavin T (ThT) as a probe, whose fluorescence intensity increases upon binding to amyloid fibrils.[52–54] $A\beta_{1\text{-}40}$ was incubated in the absence or presence of 10 molar excess of peptides **2**, **3**, and **6**-**10** at 37 °C for 24 h and ThT fluorescence intensity was recorded periodically (SI Figure S14). Reference proline-containing peptide **2** and the sulfamidate-containing peptide **8** showed statistically significant inhibition of Aβ fibrillation (74% and 62%, respectively), whereas the other peptides (**3**, **6**, **7**, **9**, and **10**) showed no inhibition (Figure 5A).

The inhibition of $A\beta_{1\text{-}40}$ aggregation was then evaluated using lower amounts of peptides (1:5 and 1:2 molar ratios, Figure 5B and SI Figure S14, S15), showing that sulfamidate-containing peptide **8** was still able to significantly inhibit the fibrillation at a 5-molar excess (79%) in a dose-dependent manner. Another way to qualitatively study amyloid fibrillation is analyzing the conformation of $A\beta_{1\text{-}40}$ after incubation by CD in the absence and presence of additives.[55] When incubating $A\beta_{1\text{-}40}$ with 2 molar excess of peptide **8** at 37 °C for 24 h, the characteristic β-sheet profile shifted to a random coil, suggesting aggregation inhibition (Figure 5C and SI Figure S16). This behavior, which is consistent with the outcome of the ThT fluorescence experiments, was maintained after incubating for 7 days (Figure 5D and SI Figure S17). Overall, these results suggest that the non-extended conformation of sulfamidate-containing peptide **8** is conserved in the presence of $A\beta_{1\text{-}40}$, thus disrupting amyloid aggregation.

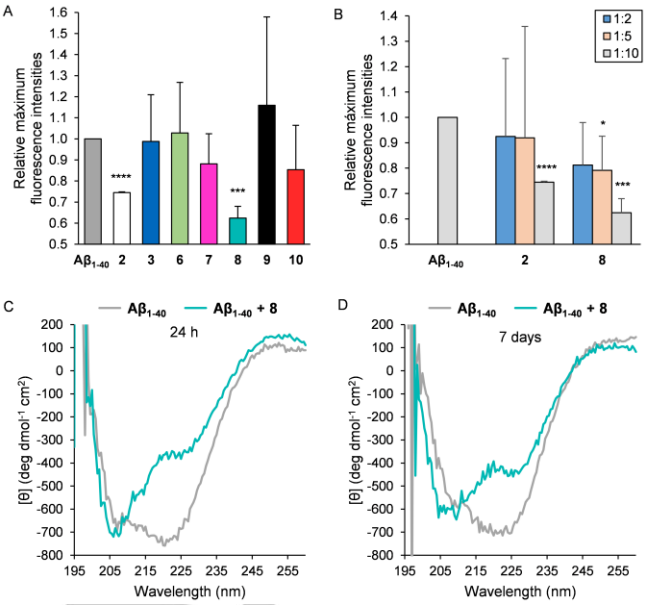

Figure 5. In vitro activity of peptides **2, 3,** and **6-10**. A) Relative maximum fluorescence intensities obtained from the ThT fluorescence assay upon incubation of $A\beta_{1\text{-}40}$ (15 μM) with and without 10 molar excess of each peptide at 37 °C for 24 h. B) Relative maximum fluorescence intensities obtained from the ThT fluorescence assay upon incubation of $A\beta_{1\text{-}40}$ (15 μM) with and without 2, 5 or 10 molar excess of peptides **2** and **8** at 37 °C for 24 h. All the samples were measured three times and the average value was used. The asterisks denote statistically significant differences (* $p \leq 0.05$, *** $p \leq 0.001$, **** $p \leq 0.0001$). C and D) Circular dichroism spectra of $A\beta_{1\text{-}40}$ incubated in the absence (grey) or presence of 2 molar excess of peptide **8** (green) at 37 °C for 24 h (C) or 7 days (D).

Model for amyloid inhibition mechanism. Saturation transfer difference (STD) NMR experiments[56–58] were performed on sulfamidate-containing peptides in complex with freshly prepared samples containing a mixture of monomers and oligomers of $A\beta_{1\text{-}42}$,[59] in order to determine which residues of the inhibitors interact with the protein. N-unprotected peptides **3** and **7** were stable enough under the experimental conditions to obtain good quality STD NMR spectra and the 2D spectra required for peptide resonances assignments. According to STD spectra, these peptides exhibited weak binding mainly through the aromatic rings of both Phe residues, as well as the Ala residue in the case of peptide **7** and, to a lesser extent, the sulfamidate moiety (SI Figure S18, S19).

With all this experimental information in hand, a computational model for the interactions between the most active peptide **8** and $A\beta_{1\text{-}40}$ at early stages of aggregation[40] was developed (see SI). Molecular dynamics (MD) simulations showed that peptide **8** preferably interacts non-specifically with the hydrophobic C-terminus of the $A\beta_{1\text{-}40}$ monomer (residues 30-35, AIIGLM), mainly through van der Waals interactions (SI Figs. S20-S21 and Table S6). In agreement with the observations from STD experiments, this suggests that peptide **8** might not exert its inhibiting action at the pre-nucleation stage, at which β-pleated content is lower than in fibrils; at best, it could delay the initial aggregation by protecting the C-terminus through non-specific interactions.[60]

We then considered the interaction of peptide **8** with models of Aβ oligomers, to assess whether the inhibitor can specifically target the β-rich structure of multimeric Aβ species. Despite recent advances in NMR and cryo-EM techniques, the structure of soluble Aβ oligomers is still elusive owing to their plasticity

and polymorphism.[61,62] For this reason, we decided to study the interaction of peptide **8** with a minimalistic Aβ aggregate model (Aβ-*dim*) presenting mixed features of low-weight Aβ oligomers and high-molecular weight aggregates, i.e. a pronounced flexibility and parallel β-strand motifs (SI Figure S22,S23). We hypothesized that peptide **8** could bind Aβ-*dim* through: i) *capping*, i.e. being incorporated into an extreme of the β-sheet; ii) *intercalation*, i.e. being incorporated in the middle of a β-sheet, breaking to some extent the oligomer organization; iii) *insertion*, i.e. a pose where peptide **8** is perpendicular to the β strands and sandwiched between the β sheets (Figure 6A). In our simulations, peptide **8** spontaneously assumed three binding modes. Intercalation of peptide **8** in the *C*-terminus region of Aβ-*dim* creates a stable hydrogen bond network with Gly38, Gly39 and Val40 (Figure 6B and SI Figure S24), as well as a destabilizing effect which propagates over the dimer architecture leading to a loss of β content, particularly in the otherwise highly structured LVFFA sequence (SI Figure S25). Capping has been observed in both a parallel (P) and anti-parallel (AP) configuration, produced hydrophobic interactions between Phe2 and Phe3 of peptide **8** and the hydrophobic core of Aβ, as well as a salt bridge between Glu5 of peptide **8** and Lys16 of one of the strands (SI Figure S26-28). Finally, in the insertion binding pose, the aromatic rings of peptide **8** interact with the hydrophobic zipper, competing for the non-polar contacts between the two β-sheets and weakening the β structure in the C-terminus region of Aβ-*dim*, particularly between residues 30 and 35 (SI Figure S29).

Stronger binding affinities have been estimated for the capping and intercalation mode (SI Table S7), suggesting that inhibition takes place through a combination of these two mechanisms that hinder templating and recruitment of further Aβ units.

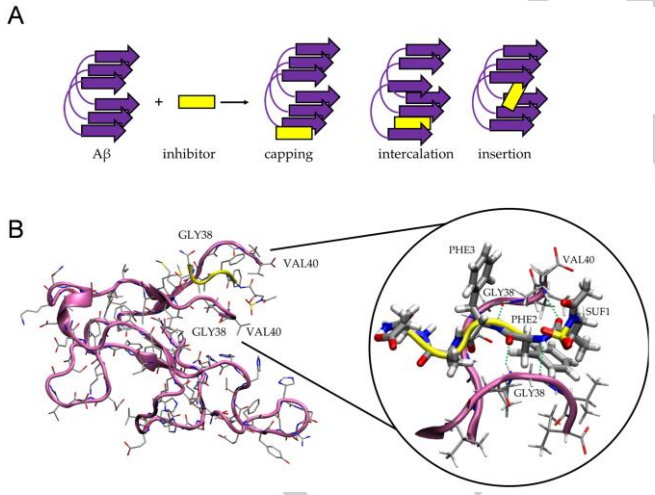

Figure 6. MD simulation of the **8**-A*β-dim* system. A) Schematic representation of the three hypothesized mechanisms of inhibition. B) Structural model of peptide **8** intercalated into *Aβ-dim* extracted from the simulation.

Conclusion

The five-membered cyclic sulfamidate derived from α-methylisoserine, when incorporated in small peptides, confers a conformational rigidity to the adjacent residues. The resulting peptides adopt mostly folded conformations in the gas phase, solid state and in aqueous solution due to electrostatic interactions involving the sulfamidate moiety. The stability of this non-extended conformation was proven *in vitro* by assays of Aβ aggregation inhibition, demonstrating the β-sheet breaker capacity of sulfamidate-containing peptide **8**. Finally, an inhibition mechanism has been proposed to elucidate how sulfamidate-containing peptides might exert β-sheet breaker activity preventing the recruitment of further Aβ into the growing fibril.

Experimental Section

General protocol for microwave-assisted solid-phase peptide synthesis (MW-SPPS): The synthesis of all the peptides was automatedly performed in a Liberty Microwave (CEM Corporation, Mathews, NC) synthesizer. Rink Amide MBHA resin (0.05, 0.10, or 0.25 mmol) was dwelled with *N*,*N*-dimethylformamide for 5 min. DIC/Oxyma Pure® were used as coupling agents, a 20% (v/v) solution of piperidine in DMF for Fmoc deprotection, and a 1:2 mixture of acetic anhydride (Ac_2O) and pyridine for the final acetylation. Natural Fmoc-protected amino acids (5.0 equiv.) were coupled using the standard protocol. Sulfamidate building block **1** (5.0 equiv.) was coupled using Oxyma Pure® (5.5 equiv.) and DIC (20.0 equiv.) in DMF (2 mL) assisted by microwave radiation at 75 ºC for 20 min. Fmoc-Leu-OH was manually coupled to the *N*-terminus of sulfamidate **1** using the optimized conditions shown in **Table S2** (entry 3). Ac-Leu-OH was manually coupled to the *N*-terminus of sulfamidate **1** using DIC/DIPEA in DMF at 25 ºC for 16 h. Peptides were detached from the resin and acid-sensitive sidechain protecting groups were cleaved by using a solution of trifluoroacetic acid (TFA)/triisopropylsilane (TIS)/H_2O (95:2.5:2.5) for 1 h at 25 ºC. Peptides were then precipitated with cold diethyl ether and centrifuged, to afford the crude derivatives. Reaction crudes were analysed using a Waters 1525 system equipped with a diode array detector (210/254 nm) using the analytical Phenomenex Luna® C18(2) column (5 µm, 250 mm × 4.6 mm) with a flow rate of 1.0 mL/min (linear gradient 5-95% B over 60 min). Peptides were purified using a Waters 2695 system equipped with a dual absorbance detector (210/254 nm) using the semi-preparative Phenomenex Luna® C18(2) column (10 µm, 250 mm × 21.2 mm) and, with a flow rate of 10 mL/min (linear gradient 2-80% B over 40 min or 2-100% B over 50 min). A: H_2O + 0.1% TFA. B: MeCN.

Synthesis of compound 8: Peptide **8** (Ac-**1**-Phe-Phe-Ala-Glu-NH_2) was synthesized and purified following the general protocol described above (18 mg, 0.025 mmol, 49% global yield from 0.05 mmol resin). Semi-preparative HPLC retention time: 30.03 min.

Spectral data for compound 8: HRMS (ESI) m/z = 739.2369, calculated for $C_{32}H_{40}N_6O_{11}SNa$ (MNa^+) = 739.2368. ^{1}H NMR (300 MHz, CD_3OD) δ (ppm): 1.37 (d, 3H, *J* = 7.2 Hz, C*H*$_3$ of Ala), 1.46 (s, 3H, C*H*$_3$), 1.91-2.07 (m, 1H, C*H*$_2$β of Glu), 2.09-2.24 (m, 1H, C*H*$_2$β of Glu), 2.35 (s, 3H, Ac), 2.39-2.49 (m, 2H, C*H*$_2$γ of Glu), 2.80-3.03 (m, 2H, C*H*$_2$ of Phe1, C*H*$_2$ of Phe2), 3.13-3.25 (m, 2H, C*H*$_2$ of Phe1, C*H*$_2$ of Phe2), 3.97 (d, 1H, *J* = 10.7 Hz, C*H*$_2$ of **1**), 4.29 (q, 1H, *J* = 7.1 Hz, C*H*α of Ala), 4.34-4.41 (m, 1H, C*H*α of Glu), 4.55 (d, 1H, *J* = 10.7 Hz, C*H*$_2$ of **1**), 4.58-4.65 (m, 1H, C*H*α of Phe2), 4.68-4.79 (m, 1H, C*H*α of Phe1), 7.13-7.37 (m, 10H, Arom). ^{1}H NMR (400 MHz, H_2O/D_2O 9:1, pH 5.7, amide region) δ (ppm): 7.84 (d, 1H, *J* = 7.5 Hz, NH of Phe2), 8.07-8.15 (m, 2H, NH of Glu, NH of Ala), 8.74 (d, 1H, *J* = 8.2 Hz, NH of Phe1). $^{13}C\{^1H\}$ NMR (75 MHz, CD_3OD) δ (ppm): 16.2 (*C*H$_3$ of Ala), 21.1 (Ac), 22.0 (*C*H$_3$), 26.9 (*C*H$_2$β of Glu), 29.9 (*C*H$_2$γ of Glu), 36.7 (*C*H$_2$ of Phe2), 36.9 (*C*H$_2$ of Phe1), 49.5 (*C*Hα of Ala), 52.1 (*C*H$_2$ of **1**), 52.5 (*C*Hα of Glu), 54.8 (*C*Hα of Phe1), 55.0 (*C*Hα of Phe2), 85.6 (NHCH$_2$*C*), 126.4, 126.5, 128.0, 128.2, 128.9, 129.0, 136.8, 166.9, 168.6 (Arom), 171.6, 171.9, 173.3, 174.8, 175.1 (*C*O).

Synthesis of compound 11: Peptide **11** (**1**-Phe-Phe-NH_2) was synthesized and purified following the general protocol described above

(89 mg, 0.188 mmol, 75% global yield from 0.25 mmol resin). No purification step was needed.

Spectral data for compound 11: HRMS (ESI) m/z = 475.1648, calculated for $C_{22}H_{26}N_4O_6S$ (MH^+) = 475.1646. ^{1}H NMR (300 MHz, CD_3OD) δ (ppm): 1.39 (s, 3H, C*H*$_3$ of **1**), 2.77-3.01 (m, 2H, C*H*$_2$ of Phe1, C*H*$_2$ of Phe2), 3.10-3.20 (m, 2H, C*H*$_2$ of Phe1, C*H*$_2$ of Phe2), 3.38 (d, 1H, *J* = 12.5 Hz, C*H*$_2$ of **1**), 3.87 (d, 1H, *J* = 12.5 Hz, C*H*$_2$ of **1**), 4.57-4.69 (m, 2H, C*H*α of Phe2, C*H*α of Phe1), 7.12-7.34 (m, 10H, Arom). ^{13}C{^{1}H} NMR (75 MHz, CD_3OD) δ (ppm): 21.8 (*C*H$_3$ of **1**), 37.1 (*C*H$_2$ of Phe2) 37.5 (*C*H$_2$ of Phe1), 51.5 (*C*H$_2$ of **1**), 54.4 (*C*Hα of Phe1), 54.7 (*C*Hα of Phe2), 89.4 (NHCH$_2$*C*), 126.4, 126.5, 128.1, 129.0, 136.6, 137.0 (Arom), 170.8, 171.4, 174.4 (*C*O). Deposition Number <url href="https://www.ccdc.cam.ac.uk/services/structures?id=doi:10.1002/chem.202202203474"> 2203474 (for **11**) </url> contains the supplementary crystallographic data for this paper. These data are provided free of charge by the joint Cambridge Crystallographic Data Centre and Fachinformationszentrum Karlsruhe <url href=" http://www.ccdc.cam.ac.uk/structures ">Access Structures service</url>.

Acknowledgements

This work was funded by the Agencia Estatal de Investigación of Spain (AEI; grants CTQ2017-89132-P to M. S., RTI2018-099592-B-C21 to J. H. B., CTQ2017-89150-R to E.C. and RTI2018-099592-B-C22 to G. J. O. and the Severo Ochoa Excellence Accreditation (SEV-2016-0644 to CIC bioGUNE), the Italian Ministry of University and Research (MIUR; grant FABBR-MIUR 2018 to C. A.), the Basque Government (grants IT1162-19 and PIBA 2018-11 to E. C.) and Universidad del País Vasco (UPV/EHU; grants PPG17/10 and GIU18/207 to E. C.), CSIC (PIC2018, LINKA20249). F.P. thanks the Ministerio de Economía y Competitividad for a Juan de la Cierva Incorporación (IJC2020-045506-I) research contract. Computational resources and laser facilities of the UPV/EHU (SGIker) and CESGA were used in this work.

Keywords: β-amino acids • β-amyloid • β-sheet breaker peptides • hybrid peptides • sulfamidates

[1] A. J. Williams, S. Chakthong, D. Gray, R. M. Lawrence, T. Gallagher, *Org. Lett.* **2003**, *5*, 811–814.
[2] A. Megia-Fernandez, J. Morales-Sanfrutos, F. Hernandez-Mateo, F. Santoyo-Gonzalez, A. Megia-Fernández, J. Morales-Sanfrutos, F. Hernández-Mateo, F. Santoyo-González, *Curr. Org. Chem.* **2010**, *15*, 401–432.
[3] M. Lorion, V. Agouridas, A. Couture, E. Deniau, P. Grandclaudon, *Org. Lett.* **2010**, *12*, 1356–1359.
[4] C. Ni, J. Liu, L. Zhang, J. Hu, *Angew. Chem. Int. Ed.* **2007**, *46*, 786–789.
[5] K. C. Nicolaou, X. Huang, S. A. Snyder, P. Bheema Rao, M. Bella, M. V. Reddy, *Angew. Chem. Int. Ed.* **2002**, *41*, 834–838.
[6] C. G. Espino, P. M. Wehn, J. Chow, J. Du Bois, *J. Am. Chem. Soc.* **2001**, *123*, 6935–6936.
[7] C. Venkateswarlu, B. Datta, S. Chandrasekaran, *RSC Adv.* **2014**, *4*, 42952–42956.
[8] J. F. Bower, J. Rujirawanich, T. Gallagher, *Org. Biomol. Chem.* **2010**, *8*, 1505–1519.
[9] J. F. Bower, J. Švenda, A. J. Williams, J. P. H. Charmant, R. M. Lawrence, P. Szeto, T. Gallagher, *Org. Lett.* **2004**, *6*, 4727–4730.
[10] S. A. Albu, K. Koteva, A. M. King, S. Al-Karmi, G. D. Wright, A. Capretta, *Angew. Chem. Int. Ed.* **2016**, *55*, 13259–13262.
[11] S. B. Cohen, R. L. Halcomb, *J. Am. Chem. Soc.* **2002**, *124*, 2534–2543.
[12] S. B. Cohen, R. L. Halcomb, *Org. Lett.* **2001**, *3*, 405–407.
[13] M. Atfani, L. Wei, W. D. Lubell, *Org. Lett.* **2001**, *3*, 2965–2968.
[14] L. Wei, W. D. Lubell, *Can. J. Chem.* **2001**, *79*, 94–104.
[15] R. E. Meléndez, W. D. Lubell, *Tetrahedron* **2003**, *59*, 2581–2616.
[16] A. G. Jamieson, N. Boutard, K. Beauregard, M. S. Bodas, H. Ong, C. Quiniou, S. Chemtob, W. D. Lubell, *J. Am. Chem. Soc.* **2009**, *131*, 7917–7927.
[17] L. Wei, W. D. Lubell, *Org. Lett.* **2000**, *2*, 2595–2598.
[18] I. García-González, L. Mata, F. Corzana, G. Jiménez-Osés, A. Avenoza, J. H. Busto, J. M. Peregrina, *Chem. Eur. J.* **2015**, *21*, 1156–1168.
[19] S. De Luca, G. Digilio, V. Verdoliva, P. Tovillas, G. Jiménez-Osés, J. M. Peregrina, *J. Org. Chem.* **2019**, *84*, 14957–14964.
[20] N. Mazo, I. García-González, C. D. Navo, F. Corzana, G. Jiménez-Osés, A. Avenoza, J. H. Busto, J. M. Peregrina, *Org. Lett.* **2015**, *17*, 5804–5807.
[21] N. Mazo, C. D. Navo, J. M. Peregrina, J. H. Busto, G. Jiménez-Osés, *Org. Biomol. Chem.* **2020**, *18*, 6265–6275.
[22] A. Lesarri, S. Mata, E. J. Cocinero, S. Blanco, J. C. López, J. L. Alonso, *Angew. Chem. Int. Ed.* **2002**, *41*, 4673–4676.
[23] A. Lesarri, E. J. Cocinero, J. C. López, J. L. Alonso, *J. Am. Chem. Soc.* **2005**, *127*, 2572–2579.
[24] L. Mata, A. Avenoza, J. H. Busto, J. M. Peregrina, *Chem. Eur. J.* **2013**, *19*, 6831–6839.
[25] C. D. Navo, N. Mazo, A. Avenoza, J. H. Busto, J. M. Peregrina, G. Jiménez-Osés, *J. Org. Chem.* **2017**, *82*, 13250–13255.
[26] C. Soto, M. S. Kindy, M. Baumann, B. Frangione, *Biochem. Biophys. Res. Commun.* **1996**, *226*, 672–680.
[27] C. Soto, E. M. Sigurdsson, L. Morelli, R. A. Kumar, E. M. Castaño, B. Frangione, *Nat. Med.* **1998**, *4*, 822–826.
[28] C. Soto, *Mol. Med. Today* **1999**, *5*, 343–350.
[29] S. Bieler, C. Soto, *Curr. Drug Targets* **2004**, *5*, 553–558.
[30] L. D. Estrada, C. Lasagna, C. Soto, in *Pharmacol. Mech. Alzheimer's Ther.*, Springer, **2007**, p. 238.
[31] M. Citron, *Nat. Rev. Drug Discov.* **2010**, *9*, 387–398.
[32] H. Amijee, J. Madine, D. A. Middleton, A. J. Doig, *Biochem. Soc. Trans.* **2009**, *37*, 692–696.
[33] C. Nerelius, A. Sandegren, H. Sargsyan, R. Raunak, H. Leijonmarck, U. Chatterjee, A. Fisahn, S. Imarisio, D. A. Lomas, D. C. Crowther, R. Strömberg, J. Johansson, *Proc. Natl. Acad. Sci. U. S. A.* **2009**, *106*, 9191–9196.
[34] C. Soto, E. M. Castano, B. Frangione, N. C. Inestrosa, *J. Biol. Chem.* **1995**, *270*, 3063–3067.
[35] S. J. Wood, R. Wetzel, J. D. Martin, M. R. Hurle, *Biochemistry* **1995**, *34*, 724–730.
[36] S. C. Li, N. K. Goto, K. A. Williams, C. M. Deber, *Proc. Natl. Acad. Sci. U. S. A.* **1996**, *93*, 6676–6681.
[37] C. Giordano, A. Masi, A. Pizzini, A. Sansone, V. Consalvi, R. Chiaraluce, G. Lucente, *Eur. J. Med. Chem.* **2009**, *44*, 179–189.
[38] A. Paul, K. C. Nadimpally, T. Mondal, K. Thalluri, B. Mandal, *Chem. Commun.* **2015**, *51*, 2245–2248.
[39] C. Giordano, A. Sansone, A. Masi, A. Masci, L. Mosca, R. Chiaraluce, A. Pasquo, V. Consalvi, *Chem. Biol. Drug Des.* **2012**, *79*, 30–37.
[40] V. Minicozzi, R. Chiaraluce, V. Consalvi, C. Giordano, C. Narcisi, P. Punzi, G. C. Rossi, S. Morante, *J. Biol. Chem.* **2014**, *289*, 11242–11252.
[41] Y. Yang, *Side Reactions in Peptide Synthesis*, Elsevier Inc., **2015**.
[42] I. León, J. Millán, E. J. Cocinero, A. Lesarri, J. A. Fernández, *Angew. Chem. Int. Ed.* **2013**, *52*, 7772–7775.
[43] C. S. Barry, E. J. Cocinero, P. Çarçabal, D. P. Gamblin, E. C. Stanca-Kaposta, S. M. Remmert, M. C. Fernández-Alonso, S. Rudić, J. P. Simons, B. G. Davis, *J. Am. Chem. Soc.* **2013**, *135*, 16895–16903.
[44] I. A. Bermejo, I. Usabiaga, I. Compañón, J. Castro-López, A. Insausti, J. A. Fernández, A. Avenoza, J. H. Busto, J. Jiménez-Barbero, J. L. Asensio, J. M. Peregrina, G. Jiménez-Osés, R. Hurtado-Guerrero, E. J. Cocinero, F. Corzana, *J. Am. Chem. Soc.* **2018**, *140*, 9952–9960.
[45] M. Carini, M. P. Ruiz, I. Usabiaga, J. A. Fernández, E. J. Cocinero, M. Melle-Franco, I. Diez-Perez, A. Mateo-Alonso, *Nat. Commun.* **2017**, 8:15195.
[46] Z. Imani, V. R. Mundlapati, G. Goldsztejn, V. Brenner, E. Gloaguen, R. Guillot, J. P. Baltaze, K. Le Barbu-Debus, S. Robin, A. Zehnacker, M. Mons, D. J. Aitken, *Chem. Sci.* **2020**, *11*, 9191–9197.

[47] G. Goldsztejn, V. R. Mundlapati, J. Donon, B. Tardivel, E. Gloaguen, V. Brenner, M. Mons, *Phys. Chem. Chem. Phys.* **2020**, *22*, 20409–20420.
[48] G. Goldsztejn, V. R. Mundlapati, V. Brenner, E. Gloaguen, M. Mons, C. Cabezas, I. León, J. L. Alonso, *Phys. Chem. Chem. Phys.* **2020**, *22*, 20284–20294.
[49] L. M. Sandvoss, H. A. Carlson, *J. Am. Chem. Soc.* **2003**, *125*, 15855–15862.
[50] A. B. Mantsyzov, O. Y. Savelyev, P. M. Ivantcova, S. Bräse, K. V. Kudryavtsev, V. I. Polshakov, *Front. Chem.* **2018**, *6*, 91.
[51] B. K. Ho, R. Brasseur, *BMC Struct. Biol.* **2005**, *5*, 14.
[52] H. Naiki, K. Higuchi, M. Hosokawa, T. Takeda, *Anal. Biochem.* **1989**, *177*, 244–249.
[53] H. LeVine, *Protein Sci.* **1993**, *2*, 404–410.
[54] H. LeVine, *Amyloid* **1995**, *2:1*, 1–6.
[55] Y. Song, E. G. Moore, Y. Guo, J. S. Moore, *J. Am. Chem. Soc.* **2017**, *139*, 4298–4301.
[56] M. Mayer, B. Meyer, *Angew. Chem. Int. Ed.* **1999**, *38*, 1784–1788.
[57] B. Meyer, T. Peters, *Angew. Chem. Int. Ed.* **2003**, *42*, 864–890.
[58] C. Airoldi, S. Merlo, E. Sironi, in *Appl. NMR Spectrosc.*, Bentham Science Publishers Ltd., **2015**, pp. 147–219.
[59] C. Airoldi, L. Colombo, C. Manzoni, E. Sironi, A. Natalello, S. M. Doglia, G. Forloni, F. Tagliavini, E. Del Favero, L. Cantù, F. Nicotra, M. Salmona, *Org. Biomol. Chem.* **2011**, *9*, 463–472.
[60] M. Ahmed, J. Davis, D. Aucoin, T. Sato, S. Ahuja, S. Aimoto, J. I. Elliott, W. E. Van Nostrand, S. O. Smith, *Nat. Struct. Mol. Biol.* **2010**, *17*, 561–567.
[61] E. E. Cawood, T. K. Karamanos, A. J. Wilson, S. E. Radford, *Biophys. Chem.* **2021**, *268*, 106505.
[62] R. Gallardo, N. A. Ranson, S. E. Radford, *Curr. Opin. Struct. Biol.* **2020**, *60*, 7–16.

10.1002/chem.202202913

WILEY-VCH

Entry for the Table of Contents

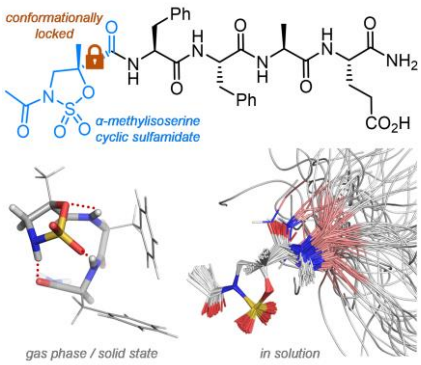

The use of a cyclic sulfamidate moiety as a β-sheet breaker element is proposed for the first time. The sulfamidate effectively locks the peptide secondary structure in a novel rigid turn both in the gas phase and solid state, which is also maintained in solution. Peptides bearing this motif show moderate amyloid-β inhibition activity.

@BilbaoChem; @CICbioGUNE; @unirioja; @upvehu